0026-895X/93/050734-07$03.00/0

MOLECULAR PHARMACOLOGY, 43:734–740

Subsecond Modulation of Formyl Peptide-Linked Guanine Nucleotide-Binding Proteins by Guanosine 5′-*O*-(3-Thio)triphosphate in Permeabilized Neutrophils

RICHARD R. NEUBIG and LARRY A. SKLAR

Departments of Pharmacology and Internal Medicine, University of Michigan Ann Arbor, Michigan 48109-0626 (R.R.N.), and Department of Cytometry, University of New Mexico, Albuquerque, 87131-5636 and Life Sciences Division, Los Alamos National Laboratory, Los Alamos, New Mexico 87545 (L.A.S.)

Received September 1, 1992; Accepted February 23, 1993

SUMMARY

Rapid activation of guanine nucleotide-binding protein (G protein)-mediated signal transduction mechanisms occurs in many tissues. The human neutrophil provides a useful model for studying the mechanisms of these fast processes. Fluorescent chemotactic tetrapeptide and pentapeptide exhibit 30–50% quenching of fluorescence upon binding to the neutrophil formyl peptide receptor, and their binding affinity is strongly regulated by the G protein G_i. We used rapid kinetic spectrofluorometric methods to study the assembly and disassembly of the ternary complex of ligand, receptor, and G protein in digitonin-permeabilized human neutrophils. Binding was studied up to 20 nM ligand, where the half-time for association was 1.2 sec. The rate constant of association was near that for diffusion-limited reactions of ligands and proteins, 2×10^7 M^{-1} sec^{-1}. The rate of uncoupling of formyl peptide receptor from G protein in the presence of high concentrations of guanine nucleotide was ≥ 5 sec^{-1} (i.e., $t_{1/2}$ of 0.14 sec). Thus, disassembly of the formyl peptide receptor-G protein complex occurs in the millisecond time domain and may be faster than the next step in the signal transduction process.

G protein-coupled receptors are involved in many cellular responses (1, 2). These range in type from proliferative to endocrine to inflammatory to neuronal (3, 4). Although many of these responses take place on the minute time scale, activation of neutrophils and stimulation of ion channels can occur within seconds or less (5, 6). A great deal is known about the structure (7) and mechanism (8) of G protein-coupled receptors. However, the precise rates and sequence of steps between binding of an agonist to a receptor and activation of the G protein are not known.

The time course of conformational changes of purified G proteins has been determined by measurements of intrinsic fluorescence (9, 10) and the kinetics of nucleotide binding and hydrolysis (11, 12). However, these *in vitro* phenomena have much slower half-times, in the range of tens of seconds to minutes. Activation of ion channels by G proteins has been monitored on the subsecond time scale by functional measurements (5). Also, the rapid kinetics of adenylyl cyclase activation by β-adrenergic receptors (13) and inhibition by α_2-adrenergic receptors (14) show time constants in the 1–2-sec^{-1} range ($t_{1/2}$, 0.69–0.35 sec). A limitation of these measurements is that they cannot assess the ligand binding state of the receptor before and during activation of the functional response.

The formyl peptide receptor in neutrophils has proven to be a very useful system for studying G protein-coupled receptor mechanisms, because direct spectroscopic measurements of the binding of fluorescein-labeled formyl peptides have been possible since 1984 (15). Because the affinity of agonist ligands for G protein-coupled receptors is greatly altered by an interaction of the receptor with the G protein, the conformational state of the receptor can be monitored by studying agonist binding (16–19).[1] In particular, a pentapeptide (F5PEP) is especially favorable for spectrofluorometric binding studies because the fluorescence of the ligand is quenched ~50% upon binding to its receptor (20).

In this report, we utilize rapid kinetic spectrofluorometric methods to address the speed of ternary complex assembly and disassembly. The guanine nucleotide-stimulated conforma-

This work was supported by National Institutes of Health Grants GM39561 (to R.R.N.) and AI19032 and RR01315 (to L.A.S.). R.R.N. is an American Heart Association/Genentech Established Investigator.

[1] R. G. Posner, S. P. Fay, M. D. Domalewski, and L. A. Sklar. Real-time spectrofluormetric analysis of ternary complex dynamics: the kinetics of signal transduction. Submitted for publication.

ABBREVIATIONS: G protein, guanine nucleotide-binding protein; F4PEP, fluorescent tetrapeptide, formyl-Met-Leu-Phe-Lys-fluorescein; F5PEP, fluorescent pentapeptide, formyl-Met-Leu-Phe-Phe-Lys-fluorescein; GTPγS, guanosine 5′-*O*-(3-thio)triphosphate; SS, sum(s) of squared residuals; HEPES, 4-(2-hydroxyethyl)-1-piperazineethanesulfonic acid; EGTA, ethylene glycol bis(β-aminoethyl ether)-*N*,*N*,*N*′,*N*′-tetraacetic acid.

tional change that results in functional uncoupling of the G protein and receptor occurs with a rate constant of ~≥5 sec^{-1} ($t_{1/2}$, 0.14 sec), the limit of resolution with currently available fluorescent ligands.

Materials and Methods

F4PEP was from Peninsula Laboratories (Belmont, CA) and F5PEP was a gift from Dr. Richard Freer (Medical College of Virginia, Richmond, VA); they were prepared as described previously (20). Digitonin was from Sigma and a fresh suspension was prepared daily for permeabilization of neutrophils as described below. Other reagents were as described previously (20).[1]

Permeabilized neutrophils or neutrophil membranes. Human neutrophils were purified by centrifugal elutriation and were permeabilized with digitonin as described previously (19).[1] The extent of permeabilization was determined by assessing the ability of guanine nucleotide to reduce F5PEP binding. Generally, if the binding was reduced by <80–90% the cells were not used. For two experiments, neutrophil membranes were prepared as described (21).

Rapid kinetic measurements. A Biologic (Grenoble, France) SFM-3 stepping motor-driven stopped-flow mixer with a cuvette light path of 2.5 mm was installed in a SLM 8000 fluorimeter. Excitation of fluorescein was at 490 nm, using a double-excitation monochromator with a slit of 8 nm to provide maximal throughput. A 520-nm bandpass filter (Corion, Holliston, MA) and a Corning 3–70 cut-off filter were used between the cuvette and the photomultiplier tube instead of the emission monochromator. The theoretical mixing dead-time of the instrument in this configuration is 3 msec. Experiments examining the quenching of fluorescein by high concentrations of an antifluorescein antibody showed an experimental dead-time of 15 msec at the flow rates used for the formyl peptide binding experiments (data not shown).[2] Data acquisition was triggered at the end of plunger movement and data were collected at 20–50-msec time intervals by using the fast time base mode of the SLM software. Although the SLM software can collect data at 1-msec time intervals, signal averaging is much improved with intervals of 20 msec or more.

Binding was measured at 37° in an intracellular binding buffer containing 100 mM KCl, 20 mM NaCl, 1 mM EGTA, 30 mM HEPES, pH 7.3, 0.1% bovine serum albumin, 1 mM phenylmethylsulfonyl fluoride (added fresh from a stock solution in ethanol), and 5 mM $MgCl_2$. Permeabilized cells or membranes were maintained on ice until they were ready to be loaded into the rapid-mixing apparatus. Samples were equilibrated for at least 5 min at 37° in the apparatus and then the data were collected as rapidly as possible. Generally, 5–15 data traces were collected for each condition. The first one or two "shots" were usually discarded because the signal was not stable, due to lack of equilibration of fluorophore throughout the apparatus.

F5PEP association kinetics. Cells (2×10^7/ml, ~1 nM receptor) in intracellular binding buffer were loaded into the rapid-mixing apparatus, equilibrated for at least 5 min at 37°, and then automatically mixed with an equal volume of buffer containing 4–40 nM F5PEP (2–20 nM final concentration). Quenching of the F5PEP fluorescence upon binding to the receptor showed the time course of ligand binding.

Guanine nucleotide-mediated dissociation of F5PEP. A concentration of 2 nM F5PEP was added to cells (2×10^7/ml) or membranes (~1 nM FPEP binding sites) on ice. The mixture was then loaded into the rapid-mixing apparatus, equilibrated for at least 5 min at 37°, and then automatically mixed with an equal volume of 2×10^{-4} M GTPγS. The increase in fluorescence reflects loss of quenching of the F5PEP fluorescence as the F5PEP dissociates from the receptor.

Double-mixing experiments. For the combined association and dissociation binding measurements (see Fig. 3), 4 nM F4PEP was mixed in the rapid-mixing apparatus with an equal volume of cells (4×10^7/ml). A 200-μl delay line was added after the first mixer so that the peptide could bind to the cells for a defined period of time before nucleotide was added. Sufficient reaction mixture was mixed to fill both the delay line and the cuvette. After the reactants had been in the delay line for 60 sec, the reaction mixture was forced into the second mixer, where an equal volume of 2×10^{-4} M GTPγS was added to initiate dissociation. Because of limitations of the data acquisition software, data from the association phase of the binding were collected in separate shots from the dissociation phase data.

Data analysis. For the association kinetics, the fluorescence decrease was fit to a one- or two-exponential decay using unweighted nonlinear least squares fits in GraphPAD InPlot (San Diego, CA). A single-exponential function adequately described the data for the time period measured (0–30 sec).

For dissociation kinetics, the increase in fluorescence was first fit to the simple exponential rise equation:

$$F = F_0 + \Delta F(1 - e^{-k_{obs}t}) \quad (1)$$

The half-time for dissociation of F5PEP was 3–4 sec, virtually identical to the value of 4 sec reported previously.[1] To determine whether there was a limiting step before the exponential dissociation of ligand began, we needed to define a model for the mechanism of the GTPγS-stimulated dissociation. Scheme 1 shows the simplest model.

$$\text{LRG} \xrightarrow{k_1} \text{LRG-GTP} \xrightarrow{k_2} \text{LR} + \text{G}^*\text{-GTP} \xrightarrow{k_3} \text{L} + \text{R} \quad \text{(scheme 1)}$$

L is the ligand, R is the receptor, LRG is the ternary complex of ligand, receptor, and G protein, and G^*-GTP is the GTP-bound active form of the G protein. k_1, k_2, and k_3 are the rate constants for the indicated steps. The G protein conformational change that results in dissociation from the receptor (governed by rate constant k_2) is simultaneous with the activation of the G protein (see Discussion for other models). At very high guanine nucleotide concentrations, the binding step, k_1, is fast.[3] We solved the differential equations for such a three-step irreversible process when the first step is fast, and the result is of the form:

$$F = F_0 + \Delta F\left[1 + \frac{k_3 e^{-k_2 t} - k_2 e^{-k_3 t}}{(k_2 - k_3)}\right] \quad (2)$$

where F_0 is the initial fluorescence level, ΔF is the amplitude of the fluorescence increase, k_2 is the rate constant for the G protein conformational change before the start of dissociation, and k_3 is the rate constant for dissociation of L once the receptor has changed to the low affinity state.[4] As k_2 increases to infinity, the lag model (eq. 2) reduces to the exponential model of eq. 1.

The dissociation data were fit to eq. 1 and then to eq. 2 with all parameters free to vary. An F test (22) was used to determine whether the more complex model (eq. 2) produced a better fit of the data than did the simpler model (eq. 1). A p value of <0.05 indicated a significant improvement.

Monte Carlo simulations. To more directly assess our ability to detect short lags, we generated simulated experimental data from eq. 2 with k_2 values of 1, 2.5, and 5 sec^{-1} ($t_{1/2}$, 0.69, 0.28, and 0.14 sec, respectively). The time interval between theoretical points was 50 msec, as in the experimental data. Random noise was added to the simulations with the InPlot program. The standard deviation of the Gaussian noise function was 25% larger than that for the experimental data (0.0067 for Figs. 5 and 7). The "simulated data" were analyzed by nonlinear least squares analysis as described above for the experimental data.

[2] Quenching of 1 nM fluorescein by antibody (1/40 dilution, final concentration) proceeded with a rate constant of 33 sec^{-1} and a half-time of 21 msec (data not shown). This demonstrates that the hardware and software are capable of measuring very fast processes.

[3] The time constant for binding would be 0.01 sec at a GTPγS concentration of 10^{-4} M if the association rate constant was 10^8 M^{-1} sec^{-1}. For 10^{-5} M it would be 0.1 sec.

[4] There was no significant difference in simulated dissociation curves if the G protein conformational change k_2 and/or the ligand dissociation k_3 was allowed to be reversible.

Results

Mixing 2 nM F4PEP with permeabilized neutrophils in the rapid-mixing apparatus resulted in a time-dependent decrease in fluorescence (Fig. 1). This decrease is due to quenching of the fluorescence of fluorescein as it interacts with the receptor. We previously showed (20)[1] that this fluorescence quenching is blocked when a nonfluorescent peptide (*t*-butoxycarbonyl-Phe-Leu-Phe-Leu-Phe) is added before the fluorescent peptide. Also, the decrease in fluorescence of F4PEP was dependent on the presence of cells, inasmuch as it did not happen in buffer alone (Fig. 1). The binding of F5PEP to permeabilized neutrophils could be easily studied at concentrations up to 20 nM (Fig. 2). The fractional decrease in fluorescence upon binding to the neutrophils decreased for higher ligand concentrations, consistent with a saturable binding process. At the highest concentration tested, 20 nM, the half-time for association was 1.2 sec and the fractional decrease in binding was only 2–3%. With the excellent reproducibility of mixing and the large number of data points, it was easy to detect even this small change in fluorescence. Consistent with binding to the receptor site, the absolute value of ΔF saturated at F5PEP concentrations of 2–6 nM. In contrast, F_0 increased linearly with ligand concentration, as expected. A second-order plot of the rate constants of binding (Fig. 2B) revealed an association rate constant of 2.7×10^7 M^{-1} sec^{-1}. This is very close to the value reported previously (19),[1] indicating that the binding measured in the stop-flow apparatus is similar to that characterized previously as being related to the formyl peptide receptor.

The major aim of this work was to determine how rapidly conformational changes can occur in this receptor-G protein system. To address that issue, we took advantage of the fact that guanine nucleotides decrease the binding affinity of chemotactic peptides. Fig. 3 illustrates a decrease in fluorescence on binding of F5PEP, followed by an increase in fluorescence upon addition of GTPγS (reflecting the decrease in F5PEP binding).

In subsequent experiments, F5PEP was added to the cells in a batch and allowed to bind, and then only the dissociation

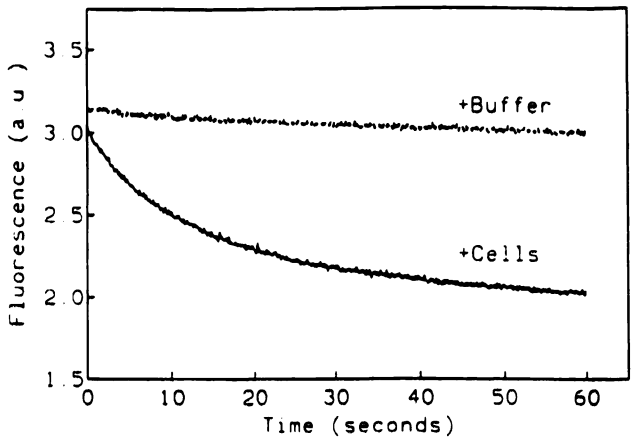

Fig. 1. Fluorescence quenching of F4PEP upon binding to the formyl peptide receptor in permeabilized neutrophils. F4PEP (2 nM, final concentration) was mixed in the Biologic SFM-3 rapid kinetic apparatus at 37° with either permeabilized neutrophils (2×10^7/ml, final concentration) (*solid line*) or buffer (*dashed line*). Data were collected at 100-msec time intervals as described in Materials and Methods. The *buffer trace* is an average of four shots and the *experimental trace* is an average of three shots. The data are expressed in arbitrary units (*a.u.*). The half-time for the fluorescence decrease in the presence of cells is 9.5 sec.

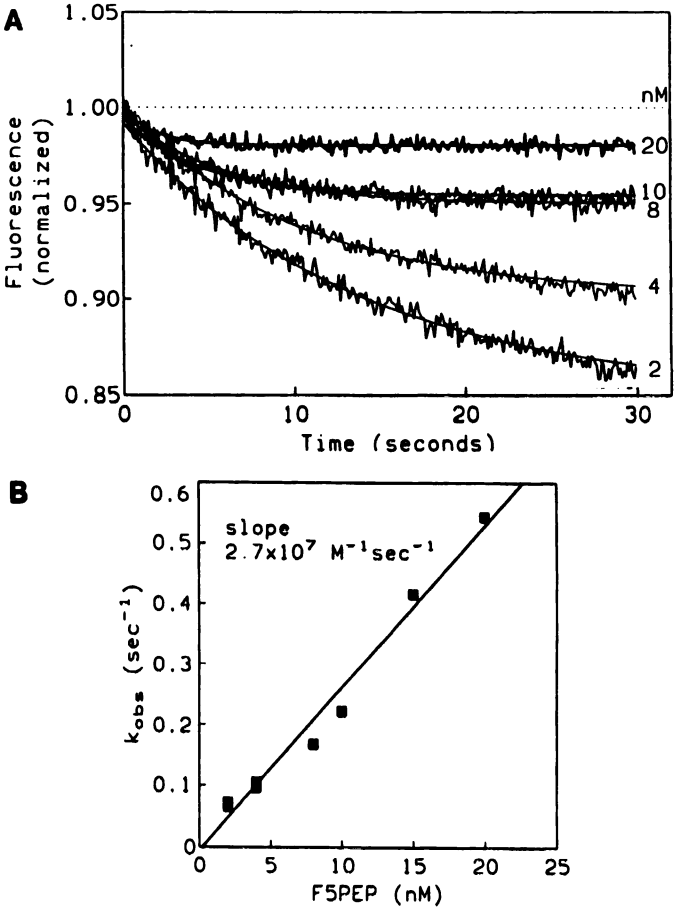

Fig. 2. Concentration dependence of F5PEP association kinetics in the rapid-mixing apparatus. A, The indicated concentrations of F5PEP were mixed with permeabilized human neutrophils (1×10^7/ml, final concentration) at 37° and the time course of fluorescence change was determined at 100-msec time intervals, as in Fig. 1. The *traces* are averages of three or four shots. *Solid lines* are nonlinear least squares fits of the data to an exponential decay. B, The rate constants for F5PEP association at each concentration were obtained from nonlinear least squares fits and are plotted. A linear regression of the secondary plot is shown with a slope of 2.7×10^7 M^{-1} sec^{-1}. This represents the association rate constant for binding of F5PEP to the receptor.

phase of the binding reaction was studied. This was done to permit more rapid collection of data and to minimize the time that cells needed to be maintained at 37° before the measurements. The increase in fluorescence upon addition of GTPγS did not occur when buffer alone was added to cells with bound F5PEP (Fig. 4). The half-time for dissociation of the ligand was 3–4 sec, which is identical to the 4-sec half-time reported previously for manual mixing experiments.[1] The dissociation half-time and percentage change in fluorescence in the rapid-mixing experiments were the same for F5PEP that had been bound for only 60 sec and for ligand that had been bound for up to 30 min.

Fig. 5, *top*, shows that guanine nucleotide-stimulated dissociation of F5PEP begins immediately and if there is any lag before the onset of dissociation it is very small. The data in this figure are an average of nine shots, and similar data were obtained in four other experiments. With the signal to noise ratio in these experiments, we could detect a lag much shorter than the half-time of dissociation. Fig. 5, *top, thin line*, shows a nonlinear least squares fit of the data to a single rising

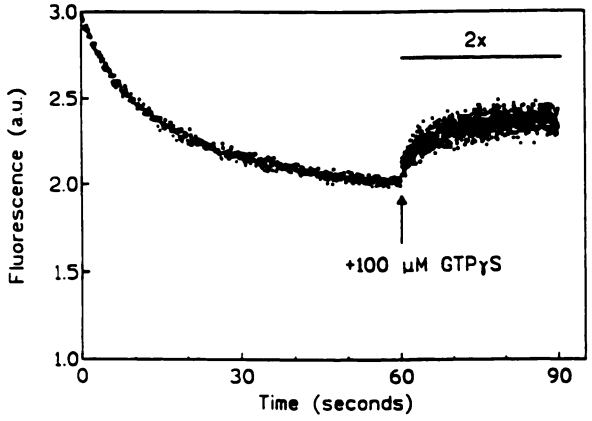

Fig. 3. Association and dissociation of F4PEP at 37°. F4PEP (4 nM) and permeabilized neutrophils (4×10^7/ml) were mixed in the rapid-mixing apparatus with a 200-μl delay line, which held the entire reaction mixture. Fluorescence measurements were triggered either immediately (association) or after 60 sec (dissociation). At 60 sec the reaction mixture was further mixed with an equal volume of buffer containing 2×10^{-4} M GTPγS and dissociation was observed. The association data are the same as in Fig. 1 and were collected every 100 msec; dissociation data were collected every 30 msec. The dissociation data were multiplied by a factor of 2 for presentation because the samples were diluted 2-fold when the GTPγS was added. The greater noise with the dissociation data was due to the lower F4PEP concentration and the decreased signal averaging that could be done with 30-msec time points. The half-time for dissociation of F4PEP was 2.8 sec. During the dissociation phase, the fluoresence does not go all the way up to the starting level because not all of the ligand dissociates upon addition of GTPγS.

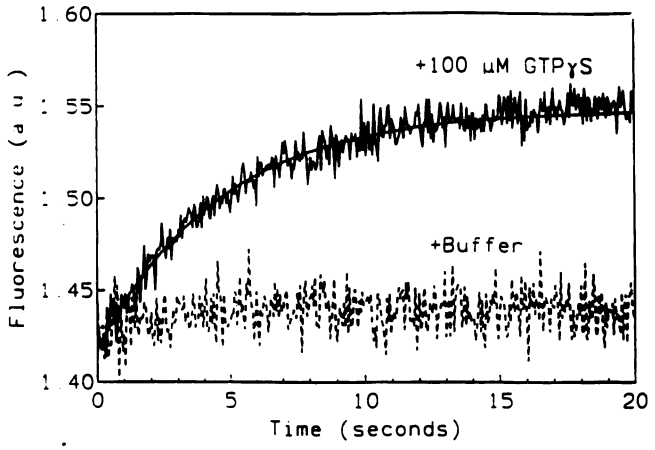

Fig. 4. Dependence of F5PEP fluorescence changes on the presence of GTPγS. F5PEP was mixed at 2 nM with permeabilized neutrophils at 2×10^7 cells/ml. The mixture was loaded into a rapid-mixing syringe and allowed to warm in the apparatus for 7 min. The mixture with bound F5PEP was then mixed with an equal volume of either buffer (*dashed line*) or 2×10^{-4} M GTPγS (*solid line*). Data were collected at 50-msec time intervals and are averages of four shots for buffer and nine shots for GTPγS. The *thin line* through the GTPγS data is a nonlinear least squares fit to eq. 1 with a half-time of 3.2 sec.

exponential function (eq. 1) with a half-time of 3.4 sec and a rate constant of 0.20 ± 0.05 sec^{-1}. We tried to directly estimate the lag time by fitting the data from the dissociation experiments to eq. 2. The best fit for the data in Fig. 5 had a k_2 of 21 ± 9 sec^{-1} ($t_{½}$, 33 msec), with a 95% confidence interval for the estimate of 2.9–40. The rate of the dissociation phase, k_3, was 0.20 ± 0.05 sec^{-1}, corresponding to a $t_{½}$ of 3.5 sec. The fit with this lag model, however, was no better than that obtained by assuming that there was no lag (i.e., eq. 1). Fig. 5, *top*, *thick*

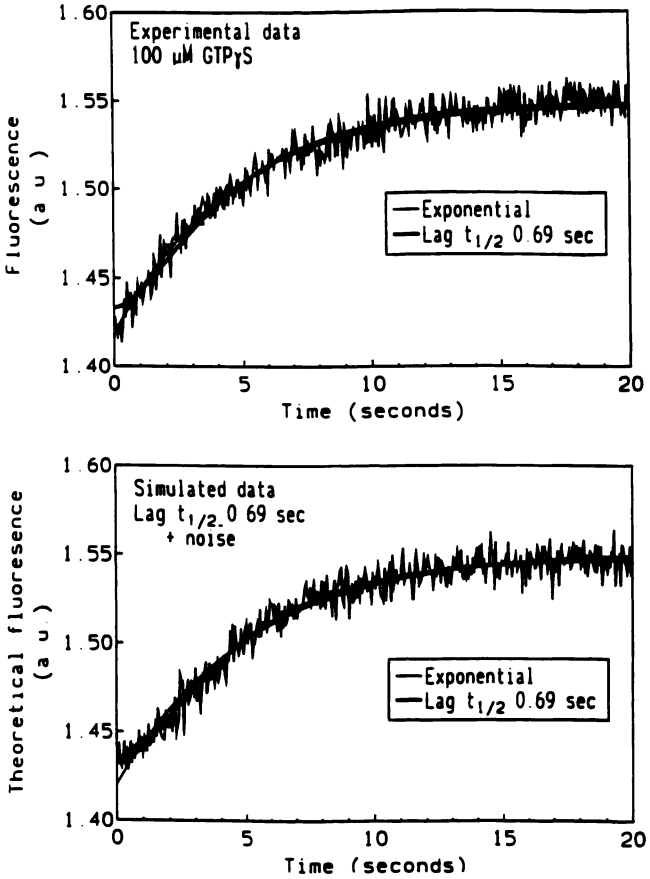

Fig. 5. Lack of lag phase in the rapid kinetics of GTPγS-stimulated dissociation of F5PEP. *Top*, the dissociation data for F5PEP from Fig. 4 were analyzed by nonlinear least squares analysis with both eq. 1 and eq. 2. *Thin line*, nonlinear least squares fit of the data to the single-exponential function (eq. 1). *Thick line*, best fit of the data when a lag with a half-time of 0.69 sec is introduced (i.e., k_2 of 1 sec^{-1} in eq. 2). *Bottom*, to determine whether a lag of 0.69 sec could be detected, simulated data were generated according to eq. 2 with a k_2 value of 1 sec^{-1} ($t_{½}$, 0.69 sec). Random noise was added that followed a Gaussian distribution with a standard deviation that matched the experimental scatter. The simulated data were then fit to the single-exponential function (*thin line*) and the lag model (*thick line*).

line, shows the best fit curve for eq. 2 when k_2 is fixed to 1 (i.e., the $t_{½}$ of the lag phase is 0.69 sec).[5] This lag phase includes the conformational change in the G protein and receptor leading to dissociation of the RG complex (see Discussion). Our ability to detect a fast G protein conformational change before ligand dissociation was examined by simulating results expected for different values of k_2. When k_2 was 1 sec^{-1} ($t_{½}$, 0.69 sec) in the simulated data, there was a clear lag phase observable (Fig. 5, *bottom*). The random error added to the simulation was of the same magnitude as the experimental error in the data set shown. We also fit the simulated data with both eq. 1 and eq. 2, and it is apparent that the fit with no lag (Fig. 5, *bottom*, *thin line*) does not reflect the simulated data.

We examined the data from the other experiments to see whether they also showed rapid onset of ligand dissociation (Fig. 6). The data were fit to both eq. 1 and eq. 2, with a $t_{½}$ of 0.69 sec, and the residuals between the fit and the experimental

[5] This is done by using eq. 2 and setting k_2 to 1 sec^{-1} ($t_{½}$, 0.69 sec). The other parameters are allowed to "float." In this case k_3 was 0.24 sec^{-1} ($t_{½}$, 2.9 sec), which is very close to the value of k for the single-exponential case.

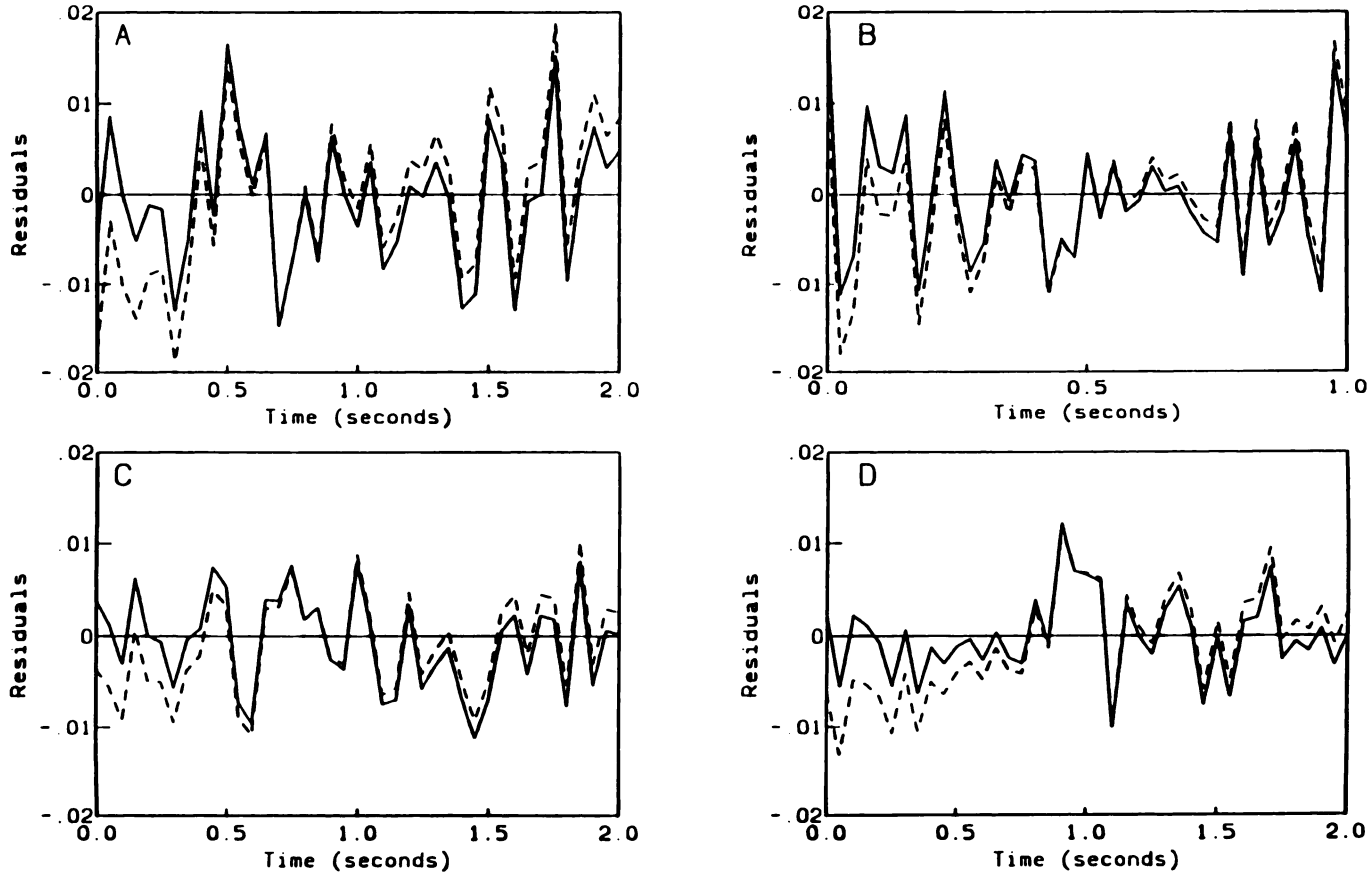

Fig. 6. Residuals analysis of F5PEP dissociation experiments. Dissociation of F5PEP in the presence of 10^{-4} M GTPγS was measured as in Figs. 4 and 5. The data were fit to either the exponential dissociation model (*solid line*) or the lag model with k_2 of 1 sec^{-1} ($t_{½}$, 0.69 sec) (*dashed line*), and then the residuals between the fitted curve and the experimental data were calculated and plotted. The data in A are from the experiment in Figs. 4 and 5. The data in B-D are from three additional experiments. All were done with permeabilized cells with 50-msec time resolution except for B, which was collected with 20-msec resolution, and C, which was done with neutrophil membranes. In each case, the no-lag case gave more uniformly distributed residuals, indicating a better fit.

data were calculated. The residuals for the fits to the single-exponential function (i.e., Fig. 6, *solid lines*, no lag) were evenly distributed above and below 0, whereas the fits with the lag phase of 0.69 sec (Fig. 6, *dashed lines*) consistently fell below 0 at the early times. In the one experiment in which the data were collected at 20-msec time intervals, to try to detect a smaller lag (Fig. 6B), the signal to noise ratio of the data was slightly worse and the deviation, while still there, was not as apparent. This analysis shows that, in all experiments, the resolution of the data was sufficient to detect a k_2 of 1 sec^{-1} ($t_{½}$, 0.69 sec) or slower.

To determine the shortest lag that we could detect with our data, we used all of the data from five experiments on four different days (each with three to nine replicate kinetic curves). We fit the data for each experiment to eq. 2 with k_2 fixed to values from 0.5 to 50 sec^{-1} ($t_{½}$, 1.4–0.014 sec). When k_2 is very large this reduces to the model with no lag at all (eq. 1). The "goodness" of the fit was measured by the SS between the curves and the data. We plotted (Fig. 7) the ratio of the SS in the full model (eq. 2) to the SS in the simple model (eq. 1). If the lag model fit the data better, we would expect the SS to decrease as k_2 gets closer to the "real" value and then to increase again as k_2 gets too large. The SS for the experimental data never got lower than that of the no-lag case. At a lag rate constant of 1 sec^{-1} ($t_{½}$, 0.69 sec) the fit was clearly worse, consistent with the conclusion of the residuals analysis in Fig. 6. Even a k_2 of 2.5 sec^{-1} ($t_{½}$, 0.28 sec) showed a consistent worsening of the fit. To further test our ability to detect a short lag, four simulations were done with k_2 equal to 2.5 sec^{-1} ($t_{½}$, 0.28 sec). The nonlinear least squares analysis and F test showed that the lag model was significantly better in two of the four simulations but not in the other two (F values of 5.7, 5.7, 1.5, and 2.8, with p values of 0.017, 0.018, 0.216, and 0.098, respectively). We plotted the ratio of SS in the full model to the SS in the simple model (Fig. 7). This clearly shows a minimum at 0.28 sec, corresponding to the value of k_2 of 2.5 sec^{-1} used in the simulations.

Thus, the conformational change of the G protein that results in agonist dissociation must occur with a half-time of <0.28 sec. Ligands with faster kinetics of dissociation from the low affinity form of the receptor would allow even faster measurements and a more precise determination of the rate of G protein conformational changes.

Discussion

In this paper, we use rapid kinetic spectrofluorometry to show that G protein conformational changes in permeabilized neutrophils occur on the 200-msec time scale or faster. This is much faster than the G protein conformational changes detected by measurements of intrinsic fluorescence of purified G

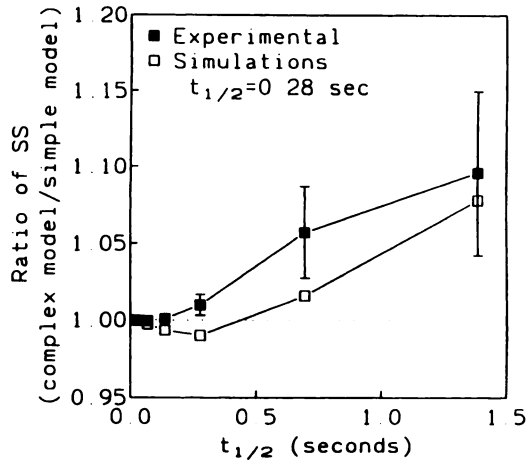

Fig. 7. Identification of the shortest lag time consistent with the dissociation data. The data from Fig. 6 and one additional experiment were fit to eq. 1 and the SS were determined. They were then fit to eq. 2 with k_2 values constrained to 50, 20, 10, 5, 2.5, 1, and 0.5 sec^{-1} (corresponding to $t_{½}$ values of 0.014, 0.035, 0.069, 0.14, 0.28, 0.69, and 1.39 sec, respectively; see Materials and Methods and Results). The SS for fits with eq. 2 were divided by the SS for the fit to eq. 1, and the ratio was plotted against k_2 (■). *Error bars*, standard error. The same type of analysis was done for simulated data with a k_2 of 2.5 sec^{-1} ($t_{½}$, 0.28 sec) (□). A smaller value for the SS ratio represents a better fit. There was no difference between the fits of the experimental data (■) for the simple model and the lag model when the lag half-times were <0.2 sec. For lag times of 0.69 or 1.4 sec, the fits were clearly worse than with the simple model for all five data sets. Even the lag time of 0.28 sec appeared to slightly worsen the fit. For the simulated data (□), the SS clearly decreases as the $t_{½}$ approaches 0.28 sec (which is the value corresponding to the simulated k_2 of 2.5 sec^{-1}). Thus, any conformational change that occurs between binding of nucleotide and the onset of F5PEP dissociation must take place on the 0.2-sec time scale or faster.

proteins (9) and even faster than the changes in transducin in the presence of rhodopsin (10).

The kinetics of G protein activation in intact cells and membranes are faster than those with purified G proteins. Thomsen and Neubig (14) showed that inhibition of adenylyl cyclase in human platelet membranes by α_2-adrenergic receptor agonists proceeded with a lag of about 1 sec at 30°. Muscarinic activation of potassium channels in heart shows similar kinetics (5). The faster rates in more intact systems may be due in part to an acceleration of GTP hydrolysis when the effector (e.g., phospholipase C or cGMP phosphodiesterase) is present (23, 24).

Our rate constant of ≥5 sec^{-1} ($t_{½}$, 0.14 sec) for the G protein conformational change appears to be faster than the rate constant of 1 sec^{-1} ($t_{½}$, 0.69 sec) for G protein activation in platelets (5, 14). At least three explanations could account for the rate of disassembly of the ternary complex in the present studies being faster than effector activation in the platelet experiments. First, it could simply be due to the higher temperature (37° in this work versus 30° for the platelet data). Second, it could be due to the different receptors involved (α_2-adrenergic receptors in platelets and formyl peptide receptors in neutrophils). However, the same $G_{\alpha i2}$ subtype is used by in both systems (25, 26). The third possibility is best discussed in relation to the model shown in scheme 2.

$$\text{LRG} \xrightarrow{k_1} \text{LRG-GTP} \begin{array}{l} \nearrow \text{G'-GTP} \xrightarrow{k_4} \text{G*-GTP} \\ \xrightarrow{k_2} \text{LR} \end{array} \xrightarrow{k_3} \text{L} + \text{R} \qquad \text{(scheme 2)}$$

In this model, there are two steps involved in G protein activation of an effector. The first is sufficient to uncouple the G protein from the receptor but the second is required for effector activation. LRG, LRG-GTP, LR, L, and R are defined in the same manner as in scheme 1. G'-GTP represents G protein that has been uncoupled from receptor but not yet fully activated. G*-GTP represents activated G protein coupled to effector. G protein activation of effector (step k_4) could be slower than the RG uncoupling (step k_2). Such fast uncoupling of G from R might be important for the catalytic function of the receptor to activate multiple G proteins. Direct spectrofluorometric measures of G protein activation will help sort out the order of these events.

The time resolution of the current data is not limited by the fluorescence technique but by the available ligands. Because F5PEP dissociates from the low affinity form of the neutrophil receptor with a half-time of 3 sec, it is hard to detect processes any faster than one tenth of that or 0.3 sec. Ironically, a lower affinity ligand with a dissociation half-time of tenths of seconds could permit detection of G protein conformational changes on the time scale of tens of milliseconds. Development of such a ligand is in progress.

The very rapid effects of GTPγS in these experiments suggest that dissociation of GDP bound to the G protein is not limiting the reactions being studied. This is consistent with the concept that the high affinity complex of ligand, receptor, and G protein involves a G protein with an empty nucleotide binding site.

The data presented here extend the limits of our knowledge concerning the speed of G protein conformational changes in a system other than the highly specialized rhodopsin-transducin case. Future studies based on this approach with more rapidly dissociating ligands and spectroscopic measures of G protein activation should reveal greater molecular detail about these important signal transduction mechanisms.

Acknowledgments

The authors thank Mark Domalewski for preparing the permeabilized neutrophils and testing the completeness of permeabilization, Dr. Richard Posner for solving the differential equations for scheme 2, and Dr. Harvey Motulsky for helpful comments. The F5PEP was a kind gift from Dr. Richard Freer of the Medical College of Virginia.

References

1. Limbird, L. E. Receptors linked to inhibition of adenylate cyclase: additional signaling mechanisms. *FASEB J.* **2**:2686–2695 (1988).
2. Freissmuth, M., P. J. Casey, and A. G. Gilman. G proteins control diverse pathways of transmembrane signalling. *FASEB J* **3**:2125–2131 (1989).
3. Spiegel, A. M. Receptor-effector coupling by G-proteins: implications for endocrinology. *Trends Endocrinol. Metab.* **1**:72–76 (1989).
4. Brown, A. M. A cellular logic for G protein-coupled ion channel pathways. *FASEB J.* **5**:2175–2179 (1991).
5. Breitwieser, G. E., and G. Szabo. Mechanism of muscarinic receptor-induced K^+ channel activation as revealed by hydrolysis-resistant GTP analogues. *J. Gen. Physiol.* **91**:469–493 (1988).
6. Yatani, A., and A. M. Brown. Rapid β-adrenergic modulation of cardiac calcium channel currents by a fast G protein pathway. *Science (Washington D. C.)* **245**:71–74 (1989).
7. O'Dowd, B. F., R. J. Lefkowitz, and M. G. Caron. Structure of the adrenergic and related receptors. *Annu. Rev. Neurosci.* **12**:67–83 (1989).
8. Gilman, A. G. G proteins: transducers of receptor-generated signals. *Annu. Rev. Biochem.* **56**:615–649 (1987).
9. Higashijima, T., K. M. Ferguson, P. C. Sternweis, E. M. Ross, M. D. Smigel, and A. G. Gilman. The effect of activating ligands on the intrinsic fluorescence of guanine nucleotide-binding regulatory proteins. *J. Biol. Chem.* **262**:752–756 (1987).
10. Guy, P. M., J. G. Koland, and R. A. Cerione. Rhodopsin-stimulated activation-deactivation cycle of transducin: kinetics of the intrinsic fluorescence response of the α subunit. *Biochemistry* **29**:6954–6964 (1990).
11. Brandt, D. R., and E. M. Ross. Catecholamine-stimulated GTPase cycle: multiple sites of regulation by β-adrenergic receptor and Mg^{2+} studied in reconstituted receptor-G_s vesicles. *J. Biol. Chem.* **261**:1656–1664 (1986).

12. Asano, T., S. E. Pedersen, C. W. Scott, and E. M. Ross. Reconstitution of catecholamine-stimulated binding of guanosine 5′-*O*-(3-thiophosphate) to the stimulatory GTP-binding protein of adenylate cyclase. *Biochemistry* **23**:5460–5467 (1984).
13. Valeins, H., T. Volker, O. Viratelle, and J. Labouesse. A quenched-flow study of a receptor-triggered second messenger response: cyclic AMP burst elicited by isoproterenol in C6 glioma cell membranes. *FEBS Lett.* **226**:331–336 (1988).
14. Thomsen, W. J., and R. R. Neubig. Rapid kinetics of α_2-adrenergic inhibition of adenylate cyclase: evidence for a distal rate limiting step. *Biochemistry* **28**:8778–8786 (1989).
15. Sklar, L. A., D. A. Finney, Z. G. Oades, A. J. Jesaitis, R. G. Painter, and C. G. Cochrane. The dynamics of ligand-receptor interactions: real-time analyses of association, dissociation, and internalization of an *N*-formyl peptide and its receptors on the human neutrophil. *J. Biol. Chem.* **259**:5661–5669 (1984).
16. De Lean, A., J. M. Stadel, and R. J. Lefkowitz. A ternary complex model explains the agonist-specific binding properties of the adenylate cyclase-coupled β-adrenergic receptor. *J. Biol. Chem.* **255**:7108–7117 (1980).
17. Kim, M. H., and R. R. Neubig. Membrane reconstitution of high-affinity α_2 adrenergic agonist binding with guanine nucleotide regulatory proteins. *Biochemistry* **26**:3664–3672 (1987).
18. Neubig, R. R., R. D. Gantzos, and W. J. Thomsen. Mechanism of agonist and antagonist binding to α_2 adrenergic receptors: evidence for a precoupled receptor-guanine nucleotide protein complex. *Biochemistry* **27**:2374–2384 (1988).
19. Fay, S. P., R. G. Posner, W. N. Swann, and L. A. Sklar. Real-time analysis of the assembly of ligand, receptor, and G protein by quantitative fluorescence flow cytometry. *Biochemistry* **30**:5066–5075 (1991).
20. Sklar, L. A., S. P. Fay, B. E. Seligmann, R. J. Freer, N. Muthukumaraswamy, and H. Mueller. Fluorescence analysis of the size of a binding pocket of a peptide receptor at natural abundance. *Biochemistry* **29**:313–316 (1990).
21. Jesaitis, A. J., J. R. Naemura, R. G. Painter, L. A. Sklar, and C. G. Cochrane. Intracellular localization of *N*-formyl chemotactic receptor and Mg^{++} dependent ATPase in human granulocytes. *Biochim. Biophys. Acta* **719**:556–568 (1982).
22. Motulsky, H. J., and L. A. Ransnäs. Fitting curves to data using nonlinear regression: a practical and nonmathematical review. *FASEB J.* **1**:365–374 (1987).
23. Bernstein, G., J. L. Blank, D.-Y. Jhon, J. H. Exton, S. G. Rhee, and E. M. Ross. Phospholipase C-β1 is GTPase-activating protein for $G_{q/11}$, its physiologic regulator. *Cell* **70**:411–418 (1992).
24. Arshavsky, V. Y., and M. D. Bownds. Regulation of deactivation of photoreceptor G protein by its target enzyme and cGMP. *Nature (Lond.)* **357**:416–417 (1992).
25. Bokoch, G. M., K. Bickford, and B. P. Bohl. Subcellular localization and quantitation of the major neutrophil pertussis toxin substrate, G_n. *J. Cell Biol.* **106**:1927–1936 (1988).
26. Gerhardt, M. A., and R. R. Neubig. Multiple G_i subtypes couple to a single effector mechanism. *Mol. Pharmacol.* **40**:707–711 (1991).

Send reprint requests to: Richard Neubig, Department of Pharmacology, University of Michigan, M6322 Medical Science Building 1, Ann Arbor, MI 48109–0626.